LANGMUIR

pubs.acs.org/Langmuir Article

Ultrasensitive Uracil-DNA Glycosylase Activity Assay and Its Inhibitor Screening Based on Primer Remodeling Jointly via Repair Enzyme and Polymerase

Yu Wang, Wenyu Sun, Jingfeng Wang, Xu Wang, Yicheng Xu, Yuanzhen Guo, Yeru Wang, Manru Zhang, Long Jiang, Su Liu, and Jiadong Huang*

Cite This: *Langmuir* 2022, 38, 3868−3875 Read Online

ACCESS | Metrics & More | Article Recommendations | Supporting Information

ABSTRACT: The development of isothermal nucleic acid amplification techniques has great significance for highly sensitive biosensing in modern biology and biomedicine. A facile and robust exponential rolling circle amplification (RCA) strategy is proposed based on primer-remodeling amplification jointly via a repair enzyme and polymerase, and uracil-DNA glycosylase (UDG) is selected as a model analyte. Two kinds of complexes, complex I and complex II, are preprepared by hybridizing a circular template (CT) with a uracil-containing hairpin probe and tetrahydrofuran abasic site mimic (AP site)-embedded fluorescence-quenched probe (AFP), respectively. The target UDG specifically binds to complex I, resulting in the generation of an AP site, followed by cleavage via endonuclease IV (Endo IV) and the successive trimming of unmatched 3′ terminus via phi29 DNA polymerase, thus producing a useable primer-CT complex that actuates the primary RCA. Then, numerous complex II anneal with the first-generation RCA product (RP), generating a complex II−RP assembly containing AP sites within the DNA duplex. With the aid of Endo IV and phi29, AFP, as a pre-primer in complex II, is converted into a mature primer to initiate additional rounds of RCA. So, countless AFPs are cleaved, releasing remarkably strong fluorescent signals. The biosensor is demonstrated to enable rapid and accurate detection of the UDG activity with an improved detection limit as low as 4.7×10^{-5} U·mL^{-1}. Moreover, this biosensor is successfully applied for UDG inhibitor screening and complicated biological samples analysis. Compared to the previous exponential RCA methods, our proposed strategy offers additional advantages, including excellent stability, optional design of CT, and simplified operating steps. Therefore, this proposed strategy may create a useful and practical platform for ultrasensitive detection of low levels of analytes in clinical diagnosis and fundamental biomedicine research.

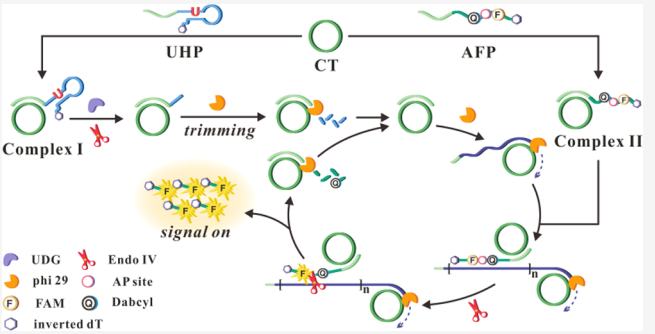

INTRODUCTION

During the last 30 years, considerable efforts have been directed toward the development of nucleic acid amplification techniques, in particular, those that can be performed isothermally, to enable the highly sensitive biosensing in modern biology and biomedicine.[1,2] The commonly used isothermal nucleic acid amplification techniques include rolling circle amplification (RCA),[3] hybridization chain reaction,[4] strand displacement amplification,[5,6] and so on. Among various isothermal amplification techniques, RCA is the earliest and most widely used that has the unique superiority of operational simplicity and high amplification efficiency.[7−9] In recent, one of the prominent development of the RCA technique is that the original linear amplification process can be converted into an exponential one by the special design of the circular templates (CTs).[10,11]

Up to now, there have been at least three groups of well-established exponential RCA methods that use nucleic acid enzymes to build more primer-CT complexes to initiate additional rounds of RCA. The main three types of exponential RCA are (1) circle-to-circle amplification, in which the first-generation RCA product (RP) can be transformed into multiple DNA monomers via restriction enzyme digestion followed by circularization through template-mediated enzymatic ligation.[12] These new CTs then can be used for a new round of RCA in the presence of a second primer.[13,14] However, the operation process of this manner is rather fussy, which involves the deactivation of DNA polymerase in the first-run RCA, the addition of additional DNA used for generating the recognition sequences for the restriction

Received: January 16, 2022
Revised: March 9, 2022
Published: March 17, 2022

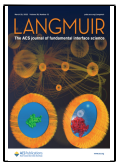

https://doi.org/10.1021/acs.langmuir.2c00115
Langmuir 2022, 38, 3868−3875

enzyme, the deactivation of restriction enzyme, and the addition of DNA ligase for the monomer-to-circle transformation. (2) Primer-generation amplification, in which the first-generation RP can be converted into multiple primer-CT complexes after hybridization with the second set of circles followed by a restriction enzyme-catalyzed cleavage reaction; thus, the obtained primer-CT complexes can be subjected to the next round of RCA.[15,16] This primer generation approach offers the advantages of operational simplicity; however, it might suffer from the troublesome hybridization between the RP and CTs because nearly all the repeating units within the RP do not have free ends to traverse the ring of CTs. (3) DNAzyme feedback amplification (DFA). Lately, the Li group reported a novel RNA-cleaving DNAzyme (RCD)-based exponential RCA strategy for biosensing through a cross-feedback mechanism.[17] This approach starts with a first-run RCA reaction that produces tandemly linked RCDs in a long-chain RP, which can cleave RNA-containing pre-primers to give rise to additional mature primers, followed by the generation of new primer-CT assemblies for the next round of RCA.[18] This DFA strategy demonstrates extremely efficient amplification and a greatly simplified operation.[19] Unfortunately, the use of RNA-containing substrates that are necessary for DFA brings on a detectable background signal resulting from substrate self-cleavage or RNases-catalyzed digestion.[20−22]

To further excavate exponential RCA techniques that are capable of overcoming the existent defects in previously reported methods, a novel type of exponential RCAmechanism termed "primer-remodeling amplification jointly via repair enzyme and polymerase (PAJRP)" has been proposed. And a PAJRP-based fluorescent strategy has been developed for the rapid and ultrasensitive detection of extremely low levels of analytes. The proposed PAJRP strategy features several aspects. Firstly, an ingeniously designed tetrahydrofuran abasic site mimic (AP site)-embedded fluorescence-quenched probe (AFP) is introduced that functions as not only the tracer but also the pre-primer used for the secondary RCA, which simplifies the operating steps and circumvents the addition of additional chemical or biological reagents for signal output. Besides, by utilizing the inverted dT modification at 3′-ends of AFP, the fluorescent background originated from DNA polymerase with 3′−5′ exonuclease activity-catalyzed substrate digestion can be effectively eliminated.[23] Secondly, a kind of repair enzyme, Endonuclease IV (Endo IV), is used to activate the polymerase-assisted primer-generation process, which avoids the use of specific sequence in CTs that is necessary for the previously reported exponential RCA methods.[24,25] At the same time, the efficiency of primer generation is exceedingly robust by cyclic cleavage of AFP via Endo IV,[26,27] endowing high amplification efficiency and excellent stability to this strategy. Finally, since the signal output is specifically controlled by the repair enzyme-assisted cleavage reaction that is dependent on the generation of the RP produced by target-triggered primary RCA, superb specificity can be achieved in the detection of analytes.[28] To demonstrate the utility of this strategy, we chose uracil-DNA glycosylase (UDG) as the model analyte. UDG, a kind of highly conserved damage repair enzyme,[29] can initiate the cellular base excision repair (BER) pathway by catalyzing the split of the *N*-glycosidic bond between the uracil and DNA backbone, liberating the impaired base and generating a flipped-out apurinic/apyrimidinic site (AP site), which is used to maintain gene stability. BER is the main DNA repair pathway for DNA base damage, and its mutation can cause gene instability and increase the risk of cancer.[30,31] Aberrant UDG activity can lead to the failure of the BER pathway, which is directly related to a variety of diseases such as cancers, human immunodeficiency, and genotypic diseases.[32] Hence, the construction of sensitive UDG activity assay methods is of crucial significance for clinical diagnosis and fundamental biomedicine research.[33−35] The results reveal that the PAJRP strategy enables rapid and accurate detection of UDG activity with an improved detection limit as low as 4.7×10^{-5} U·mL^{-1} and a widened dynamic range over 5 orders of magnitude. Furthermore, this strategy is demonstrated to be capable of UDG inhibitor screening. Therefore, the proposed strategy can establish a rapid, convenient, and highly efficient sensing system for the UDG assay and its inhibitor screening.

EXPERIMENTAL SECTION

Materials and Reagents. Sangon Biotechnology Co. Ltd. (Shanghai, China) was responsible for the synthesis and high-performance liquid chromatography-purification of all oligonucleotides in the experiment. Also, all oligonucleotide sequences were shown in Table S1. Exonuclease I (Exo I), UDG, Endo IV, exonuclease III (Exo III), phi29 DNA polymerase, 10× phi29 DNA polymerase reaction buffer, T4 DNA ligase, 10× T4 DNA ligase reaction buffer, 8-oxoguanine DNA glycosylase (hoGG1), deoxynucleotide (dNTP) solution mix, and human alkyl adenine DNA glycosylase (hAAG) were purchased from New England Biolabs (Ipswich, MA, USA). Agarose and the DNA marker (DL15000) were obtained from Takara Biotechnology Co. Ltd. (Dalian, China). Thymine DNA glycosylase (TDG) was bought from R&D System (Minneapolis, Minnesota, USA). Other reagents were all analytical grade and could be used without further purification. The solvent used in the experiment was ultrapure water obtained through a Millipore Milli-Q water purification system (Billerica, MA, USA) with resistance > 18.25 MΩ.

Apparatus. Gel electrophoresis experiments were carried out through the DYCZ-24DN electrophoresis chamber (LIUYI, China) and Bio-Rad Gel imaging system (Bio-Rad, USA). An Agilent Cary Eclipse fluorescence spectrometer (Hitachi, Japan) was used to record the fluorescence spectrum with an excitation wavelength of 486 nm. The excitation and emission slits were both set to 5 nm.

Preparation of the CT. First, 6 μL of 100 μm 5 ′-phosphorylated single-strand padlock probe, 6 μL of 100 μM ligation probe, 6 μL of 10× T4 DNA ligase reaction buffer, and 42 μL ultrapure water were added to a centrifuge tube to form a 60 μL reaction system. After that, the mixture (60 μL) was incubated at 95 °C for 5 min and then cooled to room temperature. Then, we added 3 μL 400 U·μL^{-1} T4 DNA ligase and incubated it overnight at 16 °C. The T4 DNA ligase was inactivated by heat-treating the reaction solution at 65 °C for 10 min. Afterward, 2 μL Exo I and 2 μL Exo III were added to the above ligation reaction solution and incubated at 37 °C for 2 h to digest the free probe and hybridized probe. The resulting product was incubated at 80 °C for 20 min to inactivate Exo I and Exo III and stored at 4 °C for further use. Finally, we diluted the CT I (10 μM) 100 times to obtain the CT II (100 nM).

Preparation of Complex I and Complex II. Firstly, in order to prepare Complex I, 6 μL of 100 nM CT II, 6 μL of 100 nM uracil-containing hairpin probe (UHP), 12 μL of 5× phosphate-buffered saline (PBS) buffer and 36 μL ultrapure water were added to the centrifuge tube to form a 60 μL reaction system; as for the preparation of complex II, we added 30 μL of 10 μM CT I, 6 μL of 50 μM AFP, 12 μL of 5× PBS buffer and 12 μL ultrapure water to the centrifuge tube to form a 60 μL reaction system. Afterward, the two kinds of mixture were incubated at 37 °C for 1 h.

Detection of UDG Activity. First, 3 μL of 10× phi29 DNA polymerase reaction buffer, 2 μL of 10 mM dNTPs, 3 μL of a series of concentrations of UDG, 3 μL of 5 U·μL^{-1} Endo IV, and 3 μL of 10

https://doi.org/10.1021/acs.langmuir.2c00115
Langmuir 2022, 38, 3868−3875

Scheme 1. Schematic Diagram of the Proposed Strategy for Detecting UDG Activity[a]

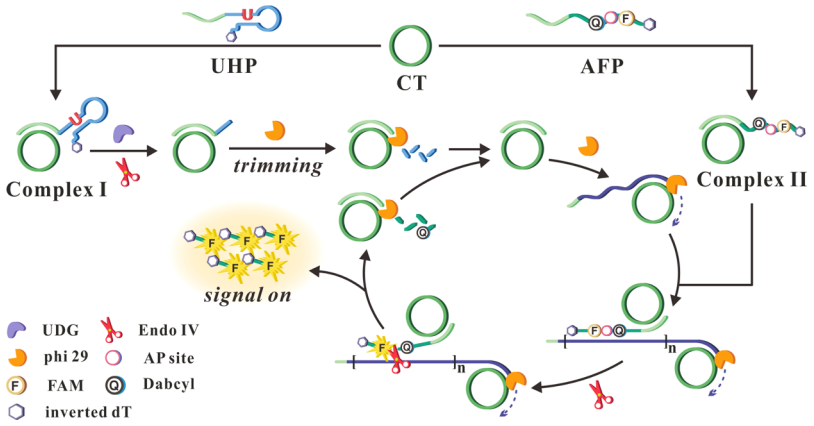

[a]U denotes the uracil deoxyribonucleotide.

U·μL^{-1} phi29 DNA polymerase were added to a centrifuge tube to form a 30 μL amplification reaction mixture. Subsequently, we added 3 μL of 10 nM complex I and 3 μL of 5 μM complex II into the amplification reaction mixture to form a mixture, which was incubated at 37 °C for 1.5 h. Finally, 70 μL ultrapure water was added into the above reaction solution and scanned with an Agilent Cary Eclipse fluorescence spectrometer. Unless otherwise stated, all UDG measurement experiments in the study were repeated three times.

Characterization of Gel Electrophoresis. For gel electrophoresis analysis of RPs, 1% agarose gel was prepared. Then, we performed an electrophoretic analysis in 50 mM TAE buffer at 135 V for 35 min. After the electrophoresis experiment, the agarose gel was visualized using the fluorescence detection of the Bio-Rad gel imaging system.

Detection of the Uracil Glycosylase Inhibitor. In order to evaluate the inhibitory effect on UDG activity, a series of concentrations of uracil glycosylase inhibitor (UGI) was chosen to improve the experimental system. A UGI can combine with UDG in a 1:1 molar stoichiometry to form a greatly tight and physiologically irreversible UGI−UDG complex. Therefore, 1 U·mL^{-1} of UDG and different concentrations of the UGI were incubated first and then incubated with 3 μL of 10 nM complex I and 3 μL of 5 μM complex II. Finally, 70 μL ultrapure water was added into the above reaction solution and scanned with an Agilent Cary Eclipse fluorescence spectrometer. All experiments were repeated three times.

Cellular UDG Assay. We cultured HeLa cells at 37 °C in Dulbecco's modified Eagle medium equipped with a 5% carbon dioxide incubator, which was supplemented with 10% fetal bovine serum and 1% penicillin−streptomycin. Then, we washed HeLa cells with PBS (pH = 7.4). And after being collected in the exponential phase of growth, HeLa cells were centrifuged at 1000 rpm for 5 min. Subsequently, HeLa cells were suspended in 100 μL of the lysis buffer and, after that, centrifuged at 12 000g at 4 °C for 20 min. For further use, the supernatant was stored at −80 °C. To carry out the inhibition analysis, HeLa cell lysis was incubated with 1 U·mL^{-1} of the UGI for 20 min at 37 °C. Finally, ultrapure water was added into the above reaction solution and scanned with an Agilent Cary Eclipse fluorescence spectrometer.

RESULTS AND DISCUSSION

Principle of the Proposed Strategy for the UDG Assay. Scheme 1 illustrates the working principle of fluorescent sensing of UDG activity. The reaction system consists of a UHP labeling with inverted dT at 3′ terminus, an AFP with inverted dT modification at 3′ end, and a CT that is complementary with either the UHP or AFP. The inverted dT modification at 3′-ends of DNA is used to prevent the substrate digestion by 3′−5′ exonuclease activity of phi29 DNA polymerase. Two kinds of complexes, namely complex I and complex II, are preprepared by hybridizing the CT with the UHP and AFP, respectively. When UDG is present, UDG can recognize the uracil base in the UHP specifically and catalyze the split of the *N*-glycosidic bond, leading to the release of the uracil and generation of the AP site (the schematic diagram is shown in Figure 2B). Immediately, Endo IV nicks the AP site inserted in the stem of the UHP, exposing the free stretching 3′ terminus that is mismatched with the CT. Then phi29 DNA polymerase successively digests unpaired bases via processive 3′−5′ exonuclease activity, converting the remaining segment of the UHP into a mature RCA primer. Subsequently, the primary RCA can be smoothly actuated with the help of phi29 and dNTP, which produces the first-generation RP with tandemly repeated DNA segments that can be complementary with the 3′ end of the AFP. Accompanied by the annealing of the protruding tail in complex II with the first-generation RP, a great many AFP-RP duplexes are formed, leading to the split of AP sites in duplexes catalyzed by Endo IV. Thus, complex II was separated from the RP. Immediately, the exposed 3′ terminus on dissociated complex II is remolded by trimming an unmatched base via 3′—5′ exonuclease activity of phi29. Accordingly, the AFP as a pre-primer was turned into a mature primer being used for feeding back into the second round of RCA. This process is termed "PAJRP". In addition, more and more complex II can bind to the first-generation RP, initiating new rounds of the "nicking−trimming−rolling" process. This process can continue to occur autonomously with repeated cycles, generating countless second-generation RPs that can bind with a growing number of complex II. As a result, a large number of AFPs are cleaved after a highly efficient exponential RCA reaction, releasing a significantly enhanced fluorescent signal. On the contrary, when the UDG is absent in the reaction system, the primary RCA is well-inhibited on the basis of the special design; thus, a negligible fluorescent signal can be obtained. Hence, the constructed PAJRP-based strategy might provide a facile and efficient tool for screening UDG activity.

Feasibility of the UDG Assay. To verify the feasibility of the suggested strategy, fluorescent responses were obtained upon monitoring UDG activity in a battery of control experiments, and the results were displayed in Figure 1. When 1 U·mL^{-1} UDG was present in the reaction system, there was a very strong emission peak at around 520 nm,

https://doi.org/10.1021/acs.langmuir.2c00115
Langmuir 2022, 38, 3868−3875

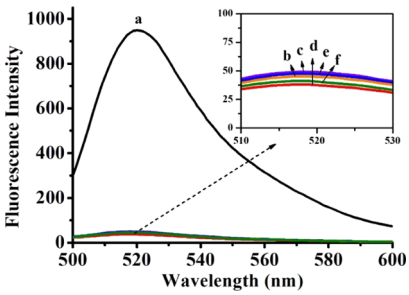

Figure 1. Fluorescent signal responses of the biosensor obtained in the assay of 1 U·mL^{-1} UDG (curve a). Curves (b–f) are the fluorescent spectral signals obtained under different conditions, which are controlled with no UDG (curve b), no phi29 (curve c), no Endo IV (curve d), nontarget enzyme TDG instead of UDG (curve e), normally paired hairpin probe (U replaced by T) instead of UHP (curve f).

manifesting numerous AFPs nicked by Endo IV, which was due to target-triggered primary RCA and was followed by an Endo IV-assisted cascade amplification reaction (curve a). In contrast, a negligible fluorescent response was obtained in the absence of UDG, demonstrating an extremely low background signal and a remarkably high signal-to-background ratio (>16-fold) for the present strategy (curve b). These data definitely displayed that the dramatically enhanced fluorescent signal was induced via specific target-assisted exponential RCA. Moreover, when phi29 (curve c) or Endo IV (curve d) was absent in the reaction system, a neglectable fluorescence emission peak was discovered, implying both enzymes were basic to the PAJRP strategy. Additionally, when incubated with the nontarget damage repair enzyme TDG instead of UDG (curve e), or the normally paired hairpin probe in place of UHP (curve f), we observed extremely weak fluorescent signals comparable to fluorescent signals of the blank sample, respectively, which verified the high specificity of this present biosensor. Furthermore, to study the effect of Endo IV-assisted feedback amplification on exponential RCA, an individual AFP was introduced to displace complex II that could combine with the first-generation RP and be circularly nicked with the aid of Endo IV; thus, a certain extent of a fluorescent response was achieved, which was decreased by 68.8% compared to that obtained in the presence of complex II (Figure S1). This data confirmed that the Endo IV-assisted feedback amplification reaction was of great help for the present exponential RCA. The above results gave direct evidence that the suggested strategy can be applied for UDG activity detection with high specificity.

Gel Electrophoresis Characterization of the UDG Assay. To excavate the amplification mechanism of the present PAJRP strategy, a series of samples were analyzed via gel electrophoresis experiments. Straightforward proofs of the ligase reaction and RCA reaction were illustrated in Figure 2A. Lane 1 was the DNA marker. When the padlock probe, ligation probe, and T4 DNA ligase were incubated together, only one bright band was observed on the top of the image (lane 2). After the addition of Exo I and Exo III, there was aband uniform with that of lane 2 (lane 3). These data confirmed that the padlock probe was circularized in the presence of the ligation probe via a T4 DNA ligase-catalyzed ligase reaction. However, when the padlock probe and ligation probe were incubated without T4 DNA ligase, no band was found on the image (lane 4), implying these probes were all digested by exonuclease. When we incubated the CT and phi29 with dNTP, it was found that an extremely bright band with low mobility appeared on the top of the image, demonstrating the commendable execution of RCA (lane 5). Additionally, we further inspected the mechanism of the UDG-assisted primer-remodeling amplification reaction, and the results were shown in Figure 2B. Lane 2 exhibited one bright band of complex I. As seen from lane 3, when we incubated complex I with UDG, there was a band similar to that of lane 2. When we incubated complex I, UDG, and Endo IV with phi29, a new band with a decreased molecular weight appeared on the image, indicating

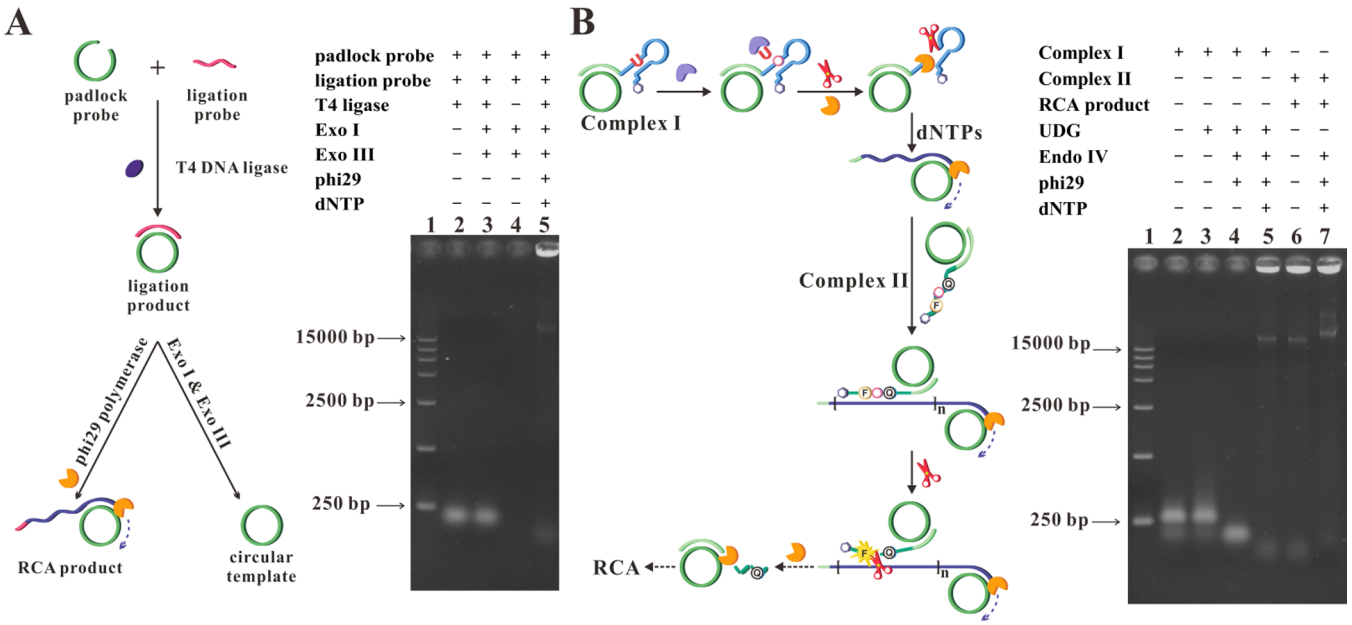

Figure 2. (A) Gel electrophoresis image of RCA reaction. (B) Gel electrophoresis image of UDG-assisted primer-remodeling amplification reaction.

https://doi.org/10.1021/acs.langmuir.2c00115
Langmuir 2022, 38, 3868–3875

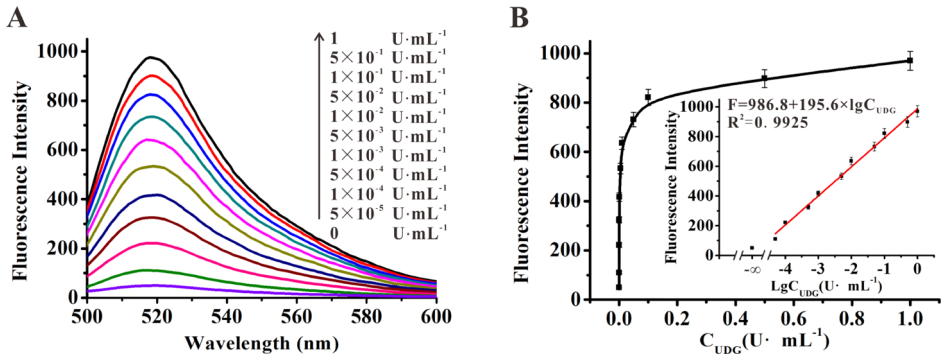

Figure 3. (A) Fluorescent intensity responses to a series of concentrations of UDG. (B) Calibration curve of fluorescent intensity values at 520 nm with varying UDG concentrations. The inset shows the relationship between the fluorescence intensity value at 520 nm and the logarithmic value of the UDG concentration.

a UDG-triggered BER and the Endo IV-assisted primer-remodeling reaction has smoothly proceeded; thus, the overhung 3′ terminus was digested that generated a mature RCA primer (lane 4). After the incubation of complex I, UDG, Endo IV, and phi29 with dNTP, we observed a bright band for the large-molecular-weight product that belongs to the first-generation RP (lane 5). After the incubation of complex II, the first-generation RP with (lane 7) and without (lane 6) Endo IV, phi29, and dNTP, it was found that the band in lane 7 was brighter than that of lane 6, which was attributed to the cyclic reaction process of "nicking−trimming−rolling" induced by the formation of a large pool of the RP. On the basis of the above results, the present exponential RCA exhibited extremely high amplification efficiency that could be used for analyzing trace amounts of analytes.

Optimization of Experimental Conditions. For the purpose of achieving the optimal analytical performance of our developed biosensor, several experimental conditions, including the phi29 DNA polymerase concentration, Endo IV concentration, concentration ratio of complex II to complex I, and reaction time, were optimized in succession. Above all, phi29 DNA polymerase is not only an essential enzyme in the RCA process but is also used for trimming immature primers into mature primers based on the 3′—5′ exonuclease activity. As shown in Figure S2, we found that the $(F - F_0)/F_0$ value gradually increased with the increasing phi29 DNA polymerase concentration and reached a plateau when the concentration was 1 U μL^{-1}. Thus, 1 U μL^{-1} was chosen as the optimal phi29 DNA polymerase concentration. Additionally, Endo IV was applied for both the BER pathway and the AP site-cleavage signal amplification in the EFA system with an optimal concentration of 0.5 U μL^{-1}, as displayed in Figure S3. Moreover, Figures S4 and S5 depicted that the optimal concentration ratio of complex II to complex I was 500 times, and the maximum value was obtained at the reaction time of 90 min, respectively. The above results lay the foundation of the further assay.

Analytical Performance of the UDG Assay. Under the optimal experimental conditions, the analytical performance of this biosensor towards UDG activity was investigated at various concentrations by fluorescence spectroscopy, and the results were demonstrated in Figure 3. It was observed from Figure 3A that the normalized fluorescent intensities increased obviously with the increase of the UDG concentration. As shown in Figure 3B, it displayed a linear dependence between the fluorescence intensity value at 520 nm and the logarithm of the UDG concentration ranging from 5×10^{-5} to 1 U·mL^{-1}. Also, the linear correlation equation is $F = 986.8 + 195.6 \times \lg C_{UDG}$ with a correlation coefficient (R^2) of 0.9925. According to the 3σ rule, we calculated the limit of detection to be 4.7×10^{-5} U·mL^{-1}. In addition, the detailed comparison between our strategy with the previously reported methods for the UDG activity assay was listed in Table S2. Our method exhibited satisfactory sensitivity and dynamic range due to the high amplification efficiency of the PAJRP strategy.

Validation of Selectivity. The selectivity of this biosensor was also validated by introducing the target UDG and several nontarget enzymes, including hOGG1, TDG, and hAAG, into the system. As shown in Figure 4, a greatly strong fluorescent

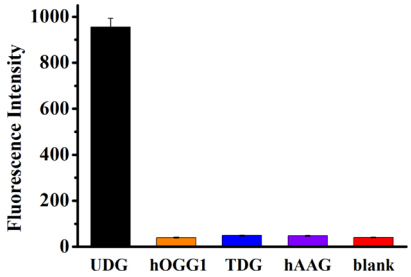

Figure 4. Plot of Fluorescence intensity obtained at 520 nm obtained in the assay of different enzymes. The UDG concentration is chosen as 1 U·mL^{-1}. The nontarget enzyme concentrations are all chosen as 50 U·mL^{-1}.

peak was observed only when the target UDG was present, whereas the responses to nontarget enzymes were comparable to that of the blank sample, indicating high specificity of this biosensor. Therefore, our developed strategy indeed provided a practical tool for UDG identification.

UDG Inhibition Assay. The screening of UDG inhibitors is of great significance for clinical diagnosis and disease therapies. Therefore, we have chosen the UGI as a model inhibitor to determine the feasibility of the suggested strategy. The inhibition reaction of UDG occurs by reversible binding of protein and the UGI at a 1:1 stoichiometry. As shown in Figure 5, as the UGI concentration increased from 1 to 25 U·mL^{-1}, the normalized fluorescence intensities at 520 nm decreased gradually. The results suggested that the approach could be used to screen UDG inhibitors and study the interaction between UDG and its inhibitors.

Cellular UDG Assay and the Inhibition Assay. To evaluate the applicability of the suggested strategy for the

https://doi.org/10.1021/acs.langmuir.2c00115
Langmuir 2022, 38, 3868−3875

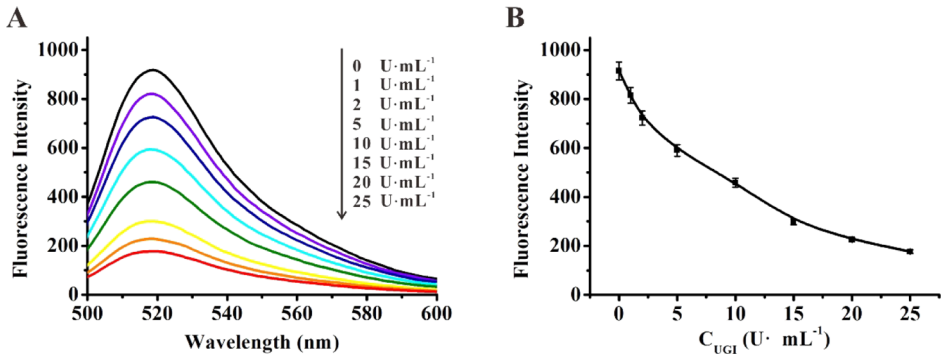

Figure 5. (A) Fluorescent responses obtained with varying concentrations of the UGI. The concentration of UDG is 1 U·mL^{-1}. (B) Calibration curve of fluorescence intensity at 520 nm upon analyzing a series of UGI concentrations. Error bars are standard deviations across three repetitive experiments.

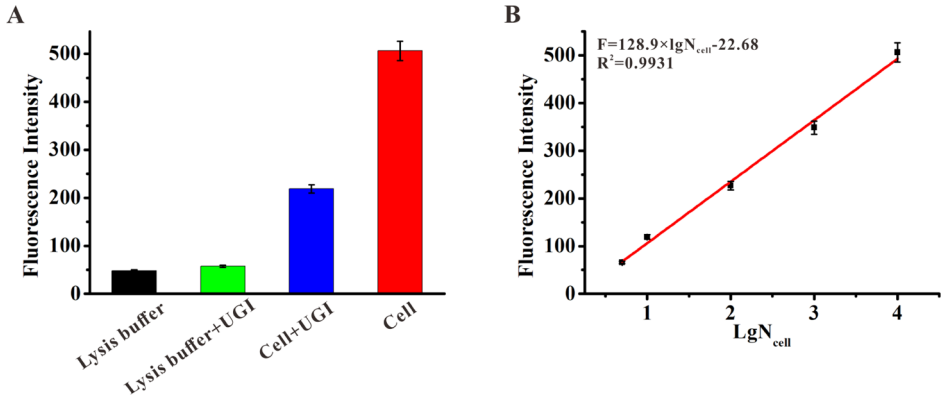

Figure 6. (A) Plot of fluorescence intensity at 520 nm obtained in the presence of lysis buffer (black column), lysis buffer + UGI (green column), cell + UGI (blue column), and cell (red column), respectively. (B) Calibration curve of the fluorescence intensity at 520 nm vs the logarithmic value of the cell number.

complicated biological matrix, the UDG activity in HeLa cells lysate was monitored. As shown in Figure 6A, very weak fluorescent signals were obtained for the lysis buffer sample (black column) or the lysis buffer sample in the presence of UGI (green column). In contrast, there was a remarkably strong fluorescent response for the HeLa cells sample (red column). For the HeLa cells in the presence of the UGI, a fluorescent intensity that decreased by 56.9% was observed (blue column), implying that the enhanced fluorescent signal was liberated by UDG instead of other components in the cell lysate. Moreover, it was found from Figure 6B that the fluorescent intensity increased monotonically upon increasing the HeLa cell numbers with the correlation equation of $F = 128.9 \times \lg N_{cell} - 22.68$ and a correlation coefficient of 0.9931, where F was the fluorescent intensity, and N was the number of HeLa cells, respectively. These results demonstrated that the biosensor could be used to monitor UDG activity in biological samples.

CONCLUSIONS

In summary, we construct a facile and robust exponential RCA strategy termed "PAJRP" for the ultrasensitive detection of UDG activity. The approach relies on the target-triggered first-generation RP that can combine with AP site-containing pre-primers; thus, the pre-primers are turned into mature primers to start additional rounds of RCA with the aid of Endo IV and phi29 DNA polymerase. The present strategy mainly features several aspects. First, Endo IV is used to enable the primer-generation process, featuring high amplification efficiency, excellent stability, and optional design of the CT of this strategy. Second, the use of a skillfully designed dual-functional AFP simplifies the operating steps and circumvents the addition of additional chemical or biological reagents for the signal output. This biosensor is shown to enable accurate and sensitive detection of UDG activity with an improved detection limit as low as 4.7×10^{-5} U·mL^{-1} and a widened dynamic range over 5 orders of magnitude. Additionally, this strategy is proved to be capable of screening inhibitors and analyzing complicated biological samples. Hence, the proposed PAJRP strategy might provide a valuable tool for detecting low levels of biomarkers in bioanalysis and contribute to disease diagnosis and fundamental biomedicine research.

ASSOCIATED CONTENT

Supporting Information

The Supporting Information is available free of charge at https://pubs.acs.org/doi/10.1021/acs.langmuir.2c00115.

Oligonucleotides sequences used in this work, research of complex II in the whole system, optimization of experiments conditions, and comparison of different methods for UDG activity determination (PDF)

AUTHOR INFORMATION

Corresponding Author

Jiadong Huang − *School of Biological Sciences and Technology, University of Jinan, Jinan 250022, P. R. China;*

https://doi.org/10.1021/acs.langmuir.2c00115
Langmuir 2022, 38, 3868−3875

orcid.org/0000-0002-0567-881X; Phone: +86-531-89736122; Email: chm_huangjd@ujn.edu.cn

Authors

Yu Wang − *School of Biological Sciences and Technology, University of Jinan, Jinan 250022, P. R. China;* orcid.org/0000-0003-2271-7371

Wenyu Sun − *School of Biological Sciences and Technology, University of Jinan, Jinan 250022, P. R. China*

Jingfeng Wang − *College of Chemistry and Molecular Sciences, Wuhan University, Wuhan 430072, P. R. China*

Xu Wang − *Shandong Institute of Metrology and Science, Jinan 250014, P. R. China*

Yicheng Xu − *School of Biological Sciences and Technology, University of Jinan, Jinan 250022, P. R. China*

Yuanzhen Guo − *School of Biological Sciences and Technology, University of Jinan, Jinan 250022, P. R. China*

Yeru Wang − *School of Biological Sciences and Technology, University of Jinan, Jinan 250022, P. R. China*

Manru Zhang − *School of Water Conservancy and Environment, University of Jinan, Jinan 250022, P. R. China*

Long Jiang − *School of Water Conservancy and Environment, University of Jinan, Jinan 250022, P. R. China*

Su Liu − *School of Water Conservancy and Environment, University of Jinan, Jinan 250022, P. R. China*

Complete contact information is available at: https://pubs.acs.org/10.1021/acs.langmuir.2c00115

Notes

The authors declare no competing financial interest.

■ ACKNOWLEDGMENTS

This work was supported by the National Natural Science Foundation of China (32072330), the Central Government Guides Local Science and Technology Development Projects of Shandong Province (YDZX20203700001955), the Jinan City "20 Items in Colleges" Funds (2019GXRC056), and the Program for Taishan Scholer of Shandong Province (ts201712048).

■ REFERENCES

(1) Zhao, Y.; Chen, F.; Li, Q.; Wang, L.; Fan, C. Isothermal amplification of nucleic acids. *Chem. Rev.* **2015**, *115*, 12491−12545.

(2) Yu, Y.; Chen, Z.; Shi, L.; Yang, F.; Pan, J.; Zhang, B.; Sun, D. Ultrasensitive electrochemical detection of microRNA based on an arched probe mediated isothermal exponential amplification. *Anal. Chem.* **2014**, *86*, 8200−8205.

(3) Zhang, K.; Lv, S.; Lin, Z.; Li, M.; Tang, D. Bio-bar-code-based photoelectrochemical immunoassay for sensitive detection of prostate-specific antigen using rolling circle amplification and enzymatic biocatalytic precipitation. *Biosens. Bioelectron.* **2018**, *101*, 159−166.

(4) Zhang, B.; Liu, B.; Tang, D.; Niessner, R.; Chen, G.; Knopp, D. DNA-Based Hybridization Chain Reaction for Amplified Bioelectronic Signal and Ultrasensitive Detection of Proteins. *Anal. Chem.* **2012**, *84*, 5392−5399.

(5) Zeng, R.; Luo, Z.; Su, L.; Zhang, L.; Tang, D.; Niessner, R.; Knopp, D. Palindromic Molecular Beacon Based Z-Scheme BiOCl-Au-CdS Photoelectrochemical Biodetection. *Anal. Chem.* **2019**, *91*, 2447−2454.

(6) Lv, S.; Zhang, K.; Zhu, L.; Tang, D. ZIF-8-Assisted NaYF4:Yb,Tm@ZnO Converter with Exonuclease III-Powered DNA Walker for Near-Infrared Light Responsive Biosensor. *Anal. Chem.* **2020**, *92*, 1470−1476.

(7) Wang, Z.-y.; Wang, M.; Zhang, Y.; Zhang, C.-y. Sensitive and label-free discrimination of 5-hydroxymethylcytosine and 5-methylcytosine in DNA by ligation-mediated rolling circle amplification. *Chem. Commun.* **2018**, *54*, 8602−8605.

(8) Wu, Z.; Lin, L.; Khan, M.; Zhang, W.; Mao, S.; Zheng, Y.; Li, Z.; Lin, J.-M. DNA-Mediated rolling circle amplification for ultrasensitive detection of thrombin using MALDI-TOF mass spectrometry. *Chem. Commun.* **2018**, *54*, 11546−11549.

(9) Liu, H.; Li, L.; Duan, L.; Wang, X.; Xie, Y.; Tong, L.; Wang, Q.; Tang, B. High specific and ultrasensitive isothermal detection of microRNA by padlock probe-based exponential rolling circle amplification. *Anal. Chem.* **2013**, *85*, 7941−7947.

(10) Ali, M. M.; Li, F.; Zhang, Z.; Zhang, K.; Kang, D.-K.; Ankrum, J. A.; Le, X. C.; Zhao, W. Rolling circle amplification: a versatile tool for chemical biology, materials science and medicine. *Chem. Soc. Rev.* **2014**, *43*, 3324−3341.

(11) Mohsen, M. G.; Kool, E. T. The discovery of rolling circle amplification and rolling circle transcription. *Acc. Chem. Res.* **2016**, *49*, 2540−2550.

(12) Zhang, X.; Zhou, Y.; Chai, Y.; Yuan, R. Double Hairpin DNAs Recognition Induced a Novel Cascade Amplification for Highly Specific and Ultrasensitive Electrochemiluminescence Detection of DNA. *Anal. Chem.* **2021**, *93*, 7987−7992.

(13) Zhang, L.-r.; Zhu, G.; Zhang, C.-y. Homogeneous and label-free detection of microRNAs using bifunctional strand displacement amplification-mediated hyperbranched rolling circle amplification. *Anal. Chem.* **2014**, *86*, 6703−6709.

(14) Yang, L.; Tao, Y.; Yue, G.; Li, R.; Qiu, B.; Guo, L.; Lin, Z.; Yang, H.-H. Highly selective and sensitive electrochemiluminescence biosensor for p53 DNA sequence based on nicking endonuclease assisted target recycling and hyperbranched rolling circle amplification. *Anal. Chem.* **2016**, *88*, 5097−5103.

(15) Murakami, T.; Sumaoka, J.; Komiyama, M. Sensitive RNA detection by combining three-way junction formation and primer generation-rolling circle amplification. *Nucleic Acids Res.* **2012**, *40*, No. e22.

(16) Wang, F.; Lu, C.-H.; Liu, X.; Freage, L.; Willner, I. Amplified and multiplexed detection of DNA using the dendritic rolling circle amplified synthesis of DNAzyme reporter units. *Anal. Chem.* **2014**, *86*, 1614−1621.

(17) Liu, M.; Zhang, Q.; Chang, D.; Gu, J.; Brennan, J. D.; Li, Y. A DNAzyme feedback amplification strategy for biosensing. *Angew. Chem., Int. Ed.* **2017**, *56*, 6142−6146.

(18) Gu, Y.; Zhang, T.-T.; Huang, Z.-F.; Hu, S.-W.; Zhao, W.; Xu, J.-J.; Chen, H.-Y. An exploration of nucleic acid liquid biopsy using a glucose meter. *Chem. Sci.* **2018**, *9*, 3517−3522.

(19) Guo, Y.; Wang, Y.; Liu, S.; Yu, J.; Wang, H.; Wang, Y.; Huang, J. Label-free and highly sensitive electrochemical detection of E. coli based on rolling circle amplifications coupled peroxidase-mimicking DNAzyme amplification. *Biosens. Bioelectron.* **2016**, *75*, 315−319.

(20) Cai, W.; Xie, S.; Zhang, J.; Tang, D.; Tang, Y. Immobilized-free miniaturized electrochemical sensing system for Pb^{2+} detection based on dual Pb^{2+}-DNAzyme assistant feedback amplification strategy. *Biosens. Bioelectron.* **2018**, *117*, 312−318.

(21) Ge, L.; Wang, W.; Li, F. Electro-grafted electrode with graphene-oxide-like DNA affinity for ratiometric homogeneous electrochemical biosensing of microRNA. *Anal. Chem.* **2017**, *89*, 11560−11567.

(22) McManus, S. A.; Li, Y. Turning a kinase deoxyribozyme into a sensor. *J. Am. Chem. Soc.* **2013**, *135*, 7181−7186.

(23) Liu, X.; Zou, M.; Li, D.; Yuan, R.; Xiang, Y. Hairpin/DNA ring ternary probes for highly sensitive detection and selective discrimination of microRNA among family members. *Anal. Chim. Acta* **2019**, *1076*, 138−143.

(24) Zeng, Y.-p.; Hu, J.; Long, Y.; Zhang, C.-y. Sensitive detection of DNA methyltransferase using hairpin probe-based primer generation rolling circle amplification-induced chemiluminescence. *Anal. Chem.* **2013**, *85*, 6143−6150.

(25) He, Y.; Yang, X.; Yuan, R.; Chai, Y. "Off" to "On" Surface-Enhanced Raman Spectroscopy Platform with Padlock Probe-Based Exponential Rolling Circle Amplification for Ultrasensitive Detection of MicroRNA 155. *Anal. Chem.* **2017**, *89*, 2866−2872.
(26) Wang, J.; Wang, Y.; Liu, S.; Wang, H.; Zhang, X.; Song, X.; Huang, J. Base excision repair initiated rolling circle amplification-based fluorescent assay for screening uracil-DNA glycosylase activity using Endo IV-assisted cleavage of AP probes. *Analyst* **2018**, *143*, 3951−3958.
(27) Wang, L.-J.; Wang, Z.-Y.; Zhang, Q.; Tang, B.; Zhang, C.-Y. Cyclic enzymatic repairing-mediated dual-signal amplification for real-time monitoring of thymine DNA glycosylase. *Chem. Commun.* **2017**, *53*, 3878−3881.
(28) Liu, X.; Song, M.; Hou, T.; Li, F. Label-free homogeneous electroanalytical platform for pesticide detection based on acetylcholinesterase-mediated DNA conformational switch integrated with rolling circle amplification. *ACS Sens.* **2017**, *2*, 562−568.
(29) Jin, Q.; Fleming, A. M.; Johnson, R. P.; Ding, Y.; Burrows, C. J.; White, H. S. Base-Excision Repair Activity of Uracil-DNA Glycosylase Monitored Using the Latch Zone of α-Hemolysin. *J. Am. Chem. Soc.* **2013**, *135*, 19347−19353.
(30) Wang, L.-j.; Ren, M.; Zhang, Q.; Tang, B.; Zhang, C.-y. Excision repair-initiated enzyme-assisted bicyclic cascade signal amplification for ultrasensitive detection of uracil-DNA glycosylase. *Anal. Chem.* **2017**, *89*, 4488−4494.
(31) Du, Y.-C.; Cui, Y.-X.; Li, X.-Y.; Sun, G.-Y.; Zhang, Y.-P.; Tang, A.-N.; Kim, K.; Kong, D.-M. Terminal Deoxynucleotidyl Transferase and T7 Exonuclease-Aided Amplification Strategy for Ultrasensitive Detection of Uracil-DNA Glycosylase. *Anal. Chem.* **2018**, *90*, 8629−8634.
(32) Du, W.; Li, J.; Xiao, F.; Yu, R.; Jiang, J. A label-free and highly sensitive strategy for uracil-DNA glycosylase activity detection based on stem-loop primer-mediated exponential amplification (SPEA). *Anal. Chim. Acta* **2017**, *991*, 127−132.
(33) Zhen, Z.; Liu, J.-W.; Wen, Q.; Wu, Z.; Jiang, J.-H. Homogeneous label-free protein binding assay using small-molecule-labeled DNA nanomachine with DNAzyme-Based chemiluminescence detection. *Talanta* **2020**, *206*, 120175.
(34) Zhang, Y.; Li, C.-c.; Tang, B.; Zhang, C.-y. Homogeneously Sensitive Detection of Multiple DNA Glycosylases with Intrinsically Fluorescent Nucleotides. *Anal. Chem.* **2017**, *89*, 7684−7692.
(35) Zhang, Y.; Li, Q.-n.; Li, C.-c.; Zhang, C.-y. Label-free and high-throughput bioluminescence detection of uracil-DNA glycosylase in cancer cells through tricyclic cascade signal amplification. *Chem. Commun.* **2018**, *54*, 6991−6994.

https://doi.org/10.1021/acs.langmuir.2c00115
Langmuir 2022, 38, 3868−3875